

# Circulation Research

JOURNAL OF THE AMERICAN HEART ASSOCIATION

American Heart  
Association®   
*Learn and Live*™

## **Impact of TASK-1 in Human Pulmonary Artery Smooth Muscle Cells**

Andrea Olschewski, Yingji Li, Bi Tang, Jörg Hanze, Bastian Eul, Rainer M. Bohle, Jochen Wilhelm, Rory E. Morty, Michael E. Brau, E. Kenneth Weir, Grazyna Kwapiszewska, Walter Klepetko, Werner Seeger and Horst Olschewski  
*Circ. Res.* 2006;98;1072-1080; originally published online Mar 30, 2006;

DOI: 10.1161/01.RES.0000219677.12988.e9

Circulation Research is published by the American Heart Association, 7272 Greenville Avenue, Dallas, TX 75214

Copyright © 2006 American Heart Association. All rights reserved. Print ISSN: 0009-7330. Online ISSN: 1524-4571

The online version of this article, along with updated information and services, is located on the World Wide Web at:

<http://circres.ahajournals.org/cgi/content/full/98/8/1072>

Data Supplement (unedited) at:

<http://circres.ahajournals.org/cgi/content/full/01.RES.0000219677.12988.e9/DC1>

Subscriptions: Information about subscribing to Circulation Research is online at  
<http://circres.ahajournals.org/subscriptions/>

Permissions: Permissions & Rights Desk, Lippincott Williams & Wilkins, a division of Wolters Kluwer Health, 351 West Camden Street, Baltimore, MD 21202-2436. Phone: 410-528-4050. Fax: 410-528-8550. E-mail:  
[journalpermissions@lww.com](mailto:journalpermissions@lww.com)

Reprints: Information about reprints can be found online at  
<http://www.lww.com/reprints>

# Impact of TASK-1 in Human Pulmonary Artery Smooth Muscle Cells

Andrea Olschewski, Yingji Li, Bi Tang, Jörg Hanze, Bastian Eul, Rainer M. Bohle, Jochen Wilhelm, Rory E. Morty, Michael E. Brau, E. Kenneth Weir, Grazyna Kwapiszewska, Walter Klepetko, Werner Seeger, Horst Olschewski

**Abstract**—The excitability of pulmonary artery smooth muscle cells (PASMC) is regulated by potassium ( $K^+$ ) conductances. Although studies suggest that background  $K^+$  currents carried by 2-pore domain  $K^+$  channels are important regulators of resting membrane potential in PASMC, their role in human PASMC is unknown. Our study tested the hypothesis that TASK-1 leak  $K^+$  channels contribute to the  $K^+$  current and resting membrane potential in human PASMC. We used the whole-cell patch-clamp technique and TASK-1 small interfering RNA (siRNA). Noninactivating  $K^+$  current performed by TASK-1  $K^+$  channels were identified by current characteristics and inhibition by anandamide and acidosis (pH 6.3), each resulting in significant membrane depolarization. Moreover, we showed that TASK-1 is blocked by moderate hypoxia and activated by treprostinil at clinically relevant concentrations. This is mediated via protein kinase A (PKA)-dependent phosphorylation of TASK-1. To further confirm the role of TASK-1 channels in regulation of resting membrane potential, we knocked down TASK-1 expression using TASK-1 siRNA. The knockdown of TASK-1 was reflected by a significant depolarization of resting membrane potential. Treatment of human PASMC with TASK-1 siRNA resulted in loss of sensitivity to anandamide, acidosis, alkalosis, hypoxia, and treprostinil. These results suggest that (1) TASK-1 is expressed in human PASMC; (2) TASK-1 is hypoxia-sensitive and controls the resting membrane potential, thus implicating an important role for TASK-1  $K^+$  channels in the regulation of pulmonary vascular tone; and (3) treprostinil activates TASK-1 at clinically relevant concentrations via PKA, which might represent an important mechanism underlying the vasorelaxing properties of prostanoids and their beneficial effect in vivo. (*Circ Res.* 2006;98:1072-1080.)

**Key Words:** pulmonary circulation ■ potassium channels ■ TASK-1 ■ treprostinil ■ hypoxic pulmonary vasoconstriction

The membrane potential of pulmonary artery smooth muscle cells (PASMC) is an important regulator of arterial tone. These cells have a resting membrane potential of approximately  $-65$  to  $-50$  mV in vitro, close to the predicted equilibrium potential for potassium ( $K^+$ ) ions. The opening of  $K^+$  channels in the PASMC membrane increases  $K^+$  efflux, which causes membrane hyperpolarization. This closes voltage-dependent  $Ca^{2+}$  channels, decreasing  $Ca^{2+}$  entry and leading to vasodilatation. Conversely, inhibition of  $K^+$  channels causes membrane depolarization,  $Ca^{2+}$  entry, cell contraction, and vasoconstriction.

Background or leak  $K^+$ -selective channels, as defined by a lack of time and voltage dependency, play an essential role in setting the resting membrane potential and input resistance in excitable cells. Two-pore domain  $K^+$  (2-PK) channels have been shown to conduct several leak  $K^+$  currents. The activity

of 2-PK channels is strongly regulated by protons, protein kinases, and hypoxia. Alteration of  $K^+$  conductance can influence cellular activity via membrane potential changes.

Both RT-PCR and Northern blot analyses performed using mammalian lung tissue identified mRNA transcripts for several 2-PK channels<sup>1,2</sup> Recently, TASK-1, a member of the 2-PK channel family was described in rabbit PASMC<sup>3</sup> and in rat pulmonary arteries.<sup>4</sup> This channel produces  $K^+$  currents that possess all of the characteristics of background conductances. The activity of TASK-1 is strongly dependent on the external pH and oxygen tension, suggesting that this particular channel might be a sensor of external pH variations and of hypoxia in pulmonary arteries.

To our knowledge, the present report is the first demonstration of the expression of TASK-1 in human PASMC (hPASMC). Our study tested the hypothesis that TASK-1

Original received June 27, 2005; resubmission received December 14, 2005; revised resubmission received March 7, 2006; accepted March 20, 2006. From the Department of Anaesthesiology (A.O., M.E.B.), Intensive Care Medicine, Medical University Graz, Austria; University of Giessen Lung Center (A.O., Y.L., B.T., J.H., B.E., R.E.M., W.S.), Medical Clinic II/V; and Department of Pathology (R.M.B., J.W., G.K.), Justus-Liebig University Giessen, Germany; Minneapolis VA Medical Center and University of Minnesota (E.K.W.); Department of Cardio-Thoracic Surgery (W.K.), Vienna University Hospital, Austria; and Division of Pulmonology (H.O.), Medical University Graz, Austria.

W.S. and H.O. are consultants for Lung RX (Satellite Beach, Fla).

Correspondence to Andrea Olschewski, Department of Anaesthesiology, Intensive Care Medicine, Medical University Graz, Auenbruggerplatz 29, A-8029 Graz, Austria. E-mail andrea.olschewski@physiologie.med.uni-giessen.de

© 2006 American Heart Association, Inc.

*Circulation Research* is available at <http://circres.ahajournals.org>

DOI: 10.1161/01.RES.0000219677.12988.e9

contributes to the  $K^+$  current and resting membrane potential by using TASK-1 small interfering RNA (siRNA). We show, moreover, that TASK-1 is sensitive to acute hypoxia and activated by treprostinil, a stable analog of prostacyclin via a protein kinase (PKA)-dependent pathway. Thus it may provide an important mechanism for the prostanoid-induced relaxation of pulmonary arteries.

## Materials and Methods

### Preparation of Human Primary Pulmonary Artery Smooth Muscle Cells and Cell Culture

Primary SMC were isolated from human pulmonary arteries from 3 unused donor lungs harvested for lung transplantation (see the online data supplement available at <http://circres.ahajournals.org>). The study protocol for tissue donation was approved by the "Ethik-Kommission am Fachbereich Humanmedizin der Justus-Liebig-Universitaet Giessen of the University Hospital Giessen" in accordance with German law and with Good Clinical Practice/International Conference on Harmonisation guidelines. Written informed consent was obtained from each individual patient or the next of kin of the patient. Cultured hPASMCM from 10 donors were purchased from Cambrex (Walkersville, Md) or from Cascade Biologics (Mansfield, UK).

### Electrophysiology

The whole-cell patch-clamp technique on hPASMCM was used as previously described to measure the resting membrane potential under current clamp and macroscopic  $K^+$  currents under voltage clamp (see the online data supplement).<sup>3,5,6</sup>

### Solutions and Chemicals

All compounds were purchased from Sigma Chemical Co (St Louis, Mo). Treprostinil was a gift from Lung RX (Satellite Beach, Fla) (see the online data supplement).

### Relative mRNA Quantification

Real-time PCR was used for relative quantification of the TASK-1, TASK-2, TASK-3, PRKCA, and PRKCE mRNA (see the online data supplement).

### Design and Transfection of siRNA for Human TASK-1

The target sequence of siRNA is localized 261 bases downstream from the start codon of human TASK-1 (GenBank accession no. AF006823). The forward and reverse strands (UCA CCG UCA UCA CCA CCA U dTdT) and (AGU GGC AGU AGU GGU GGU A dTdT) with two 5' deoxy-thymidine overhangs were commercially synthesized (Eurogentec, Seraing, Belgium) and annealed at a final concentration each of 20  $\mu$ mol/L by heating at 95°C for 1 minute and incubating at 37°C for 1 hour in annealing buffer (20 mmol/L Na-acetate, 6 mmol/L HEPES-KOH [pH 7.4], and 0.4 mmol/L Mg-acetate). Transfection of siRNA was performed at a final concentration of 40 nmol/L using Oligofectamin (Invitrogen). As a control, a random siRNA sequence (siRNA-ran: UAC ACC GUU AGC AGA CAC C dTdT) prepared as described above was used. RNA and electrophysiological measurements were performed 48 to 72 hours after transfection of siRNAs. For assessment of transfection efficiency, we used a fluorescein isothiocyanate (FITC)-conjugated siRNA (QIAGEN), the intracellular location of which was assessed by direct visualization of the FITC by fluorescence microscopy after transfection.

### Immunoprecipitation

Cultured smooth muscle cells were solubilized as described previously<sup>7</sup> in an extraction buffer supplemented with 1 mmol/L sodium orthovanadate, 10 mmol/L sodium pyrophosphate, 5 mmol/L  $\beta$ -glycerophosphate, and 50 mmol/L sodium fluoride. The TASK-1

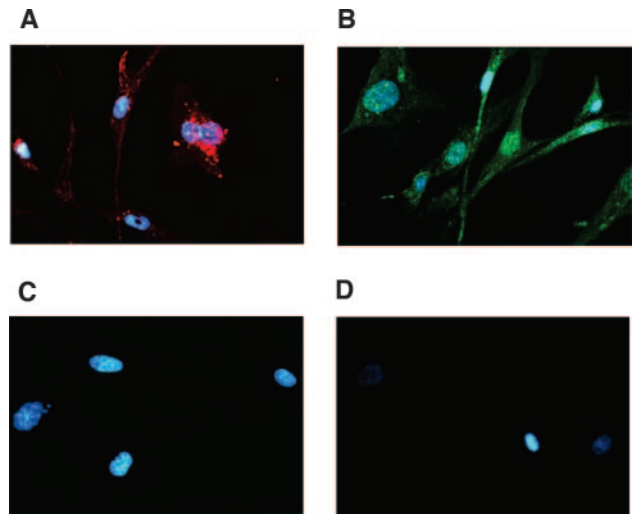


**Figure 1.** TASK-1 expression in hPASMCM. Fluorescence images of hPASMCM stained with the Alomone C-terminal TASK-1 and anti-rabbit Alexa 555 antibodies (A) or Santa Cruz N-terminal TASK-1 with anti-goat IgG-FITC antibodies (B). Staining is absent in control cells treated identically but without exposure to primary antibody, as shown by matched fluorescence (C and D, respectively).

was immunoprecipitated from cell lysates (4 hours; 4°C) using rabbit anti-TASK-1 (Alomone Labs, Jerusalem, Israel).<sup>8</sup> Antibodies were chemically coupled to protein A-Sepharose beads using a Seize Immunoprecipitation Kit (Pierce, Rockford, Ill). Immunoprecipitates were washed to a final stringency of 470 mmol/L NaCl in extraction buffer. Immunoprecipitates were resolved on a 10% Tris-Tricine SDS-PAGE gel, and blots were probed with rabbit anti-TASK-1 (1:500; Alomone Labs), mouse anti-phosphotyrosine (1:1750; Cell Signaling Technologies, Beverly, Mass), or mouse anti-phospho(Ser/Thr) (1:1000; Cell Signaling Technologies) antibodies.

### Immunofluorescence Staining

Immunofluorescence was performed as previously described, using 2 different antibodies directed against unique domains in TASK-1: the first at the amino terminus (Santa Cruz Biotechnology) and the other at residues 252 to 269 in the carboxy terminal end of the protein (Alomone Labs)<sup>3</sup> (online data supplement).

### Statistical Analysis

Numerical values are given as means  $\pm$  SE of *n* cells. Intergroup differences were assessed by a factorial analysis of variance with post hoc analysis with Fisher's least-significant difference test or Student's unpaired and paired *t* tests as appropriate. Probability values of  $<0.05$  were considered significant. The mean data at different anandamide concentrations were fitted.

## Results

### Expression of TASK-1 Channels in hPASMCM

The presence of TASK-1 protein was established with 2 anti-TASK-1 antibodies directed against the amino or carboxy terminal regions of the protein (*n*=4; Figure 1A and 1B). In contrast, staining was absent from control cells treated in the same way but without exposure to TASK-1 antibody (Figure 1C and 1D). PCR studies demonstrated the presence of TASK-1, TASK-2, and TASK-3 in human brain tissue, but only TASK-1 mRNA was detected in primary and in cultured hPASMCM as well (Figure 2A).

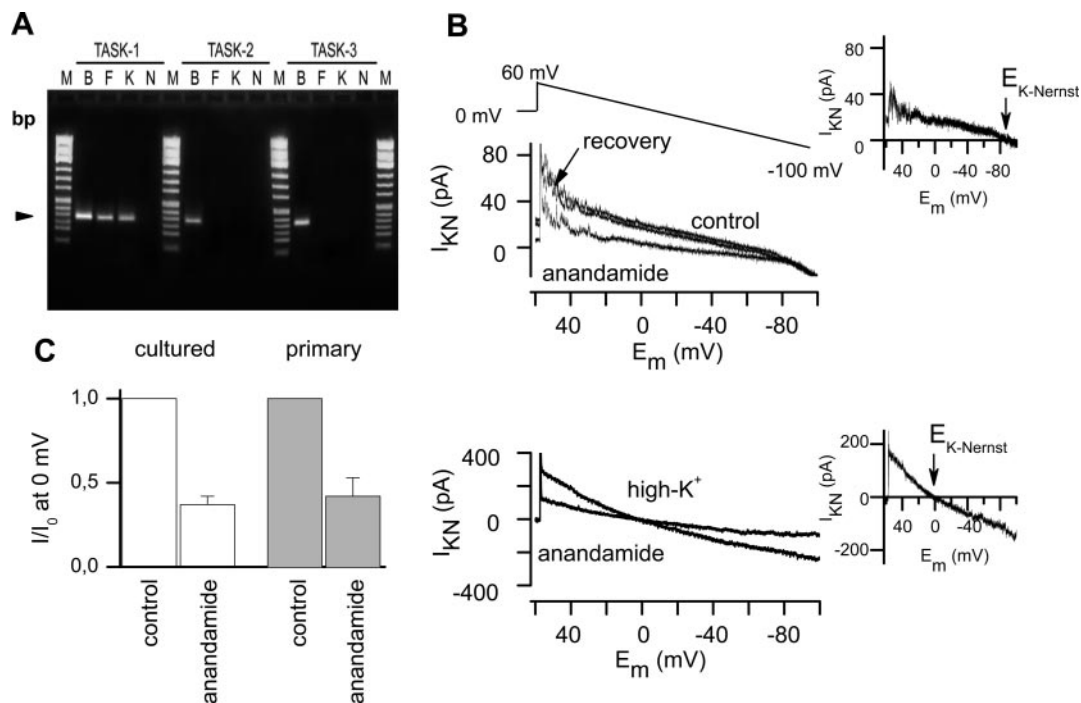


**Figure 2.**  $I_{KN}$  in primary PASMC. A, Representative gel shows mRNA expression of TASK-1 (91 bp), TASK-1 (94 bp), and TASK-3 (104 bp) in human brain (B), primary hPASM (F), and cultured hPASM (K). Only TASK-1 is expressed in primary hPASM (F) and cultured hPASM (K). Arrow indicates 100 bp; M, the molecular weight marker used to indicate the size of the PCR fragments; N, no template control. Identical results were obtained with at least 3 additional preparations of RNA. B, top, Effect of 10  $\mu\text{mol/L}$  anandamide on  $I_{KN}$  recorded during ramp, voltage protocol inset (left) and difference current trace, obtained by subtracting current amplitudes in the presence of TASK-1 blocker from those obtained under control conditions (right). Difference current reversed close to  $-84$  mV, as expected for a  $K^+$ -selective conductance under these conditions. Bottom,  $I_{KN}$  evoked under symmetrical (155  $K^+$ ) conditions by ramp in the same cell (voltage protocol above), before (high- $K^+$ ) and during application of 10  $\mu\text{mol/L}$  anandamide (left) and trace of difference currents (right). Difference current was voltage independent and reversed close to 0 mV, as expected for a  $K^+$ -selective conductance under these conditions. C, Histogram summarizing the effect of 10  $\mu\text{mol/L}$  anandamide on  $I_{KN}$  calculated at 0 mV in cultured and primary hPASM ( $n=5$  each group).  $I/I_0$  is the current in the presence of anandamide expressed as a fraction of the current before anandamide application.  $E_{K-Nernst}$  indicates Nernst equilibrium potential.

### TASK-1 Was Functionally Expressed in hPASM

Anandamide, a member of endogenous cannabinoids, was recently shown to be a direct and selective blocker of TASK-1 channels.<sup>3,9</sup> As depicted in Figure 2, application of 10  $\mu\text{mol/L}$  anandamide markedly but reversibly inhibited the noninactivating  $K^+$  current ( $I_{KN}$ ) in primary hPASM from  $16 \pm 2$  to  $6 \pm 2$  pA ( $P < 0.05$ ), recorded at 0 mV after the cells were clamped at 0 mV for least 5 minutes to inactivate voltage-dependent  $K^+$  channels. Figure 2B shows a representative recording from the holding potential of 0 mV; the voltage was stepped to 60 mV and then ramped to  $-100$  mV over a period of 1.6 seconds. The current during the ramp reflects  $I_{KN}$  parallel with a nonspecific “leak” current and reverses direction at the resting potential of the hPASM.<sup>3,5</sup> As a consequence of inhibition of the outward current, anandamide also influenced the reversal potential of the current (Figure 2B, top). The “difference” current, obtained by subtracting the current remaining in the presence of anandamide from that obtained under control conditions (Figure 2B, bottom, inset), was reversed close to  $-84$  mV, the calculated Nernst equilibrium potential for  $K^+$  under these conditions. Maintenance of a resting membrane potential in rabbit PASMC has been proposed to involve TASK-1.<sup>3</sup> Indeed, anandamide significantly depolarized hPASM ( $9 \pm 1$  mV;  $n=5$ ;  $P < 0.05$ ). Under symmetrical  $K^+$  conditions in the

same cell, anandamide caused marked inhibition of  $K^+$  current (Figure 2B, bottom). The difference current (inset) was linear and reversed at or near 0 mV, the calculated Nernst equilibrium potential for  $K^+$  under these conditions. This pharmacological and biophysical profile demonstrated the functional expression of the  $K^+$ -selective background channel TASK-1 in primary hPASM.

In cultured hPASM, a functional expression of kinetically identical  $K^+$  channels was recorded (Figure 3). The anandamide concentration-response curve for TASK-1 indicated an apparent  $IC_{50}$  of  $0.81 \pm 0.08$   $\mu\text{mol/L}$  ( $n=5$ ; Figure 3B). The effect of 10  $\mu\text{mol/L}$  anandamide was reversible (Figure 3C). It is noteworthy that the current block by anandamide recorded at 0 mV was similar in both primary and cultured hPASM (Figure 2C). Whole-cell  $K^+$  current ( $I_K$ ) in cultured hPASM was also investigated at a holding potential of  $-80$  mV. Current was activated with 250-ms depolarizing pulses from  $-80$  to  $+70$  mV in 10-mV steps. The mean current was measured during the last 150 ms of the voltage-clamp pulse and plotted against the test potential to achieve a steady-state current-voltage relationship. Conductance was obtained from linear regression of the data points between  $-60$  and 0 mV, with correlation coefficients greater than 0.95 in all cases. We focused on the anandamide sensitivity of the whole-cell current. The effect of the drug on  $I_K$  is illustrated in Figure

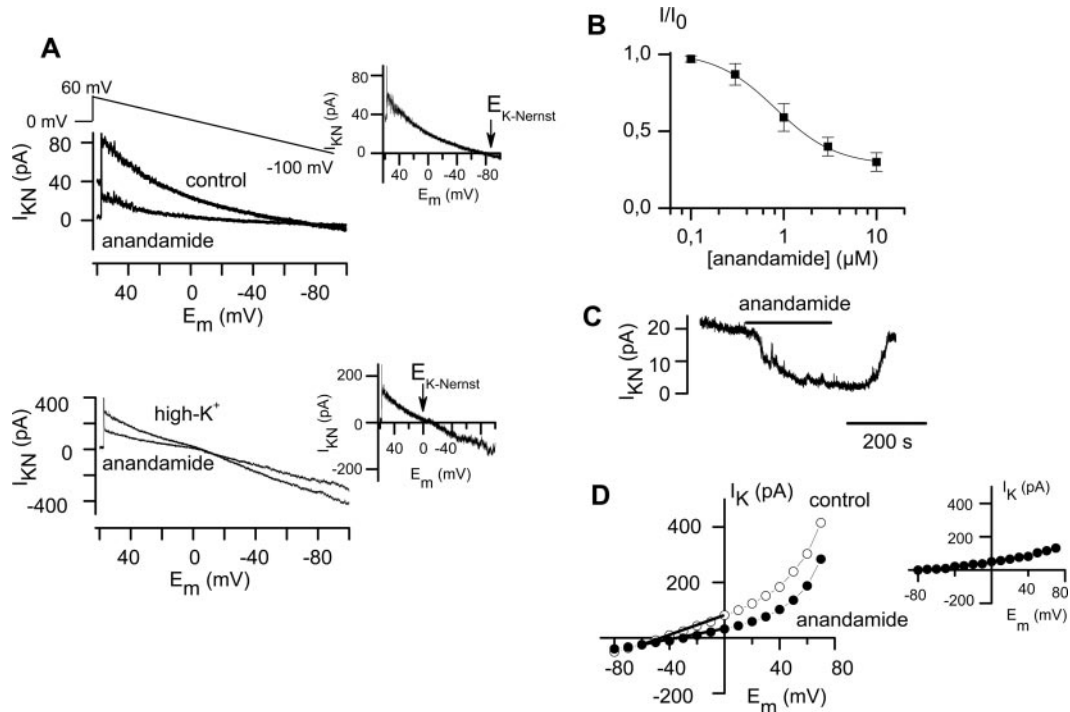


**Figure 3.**  $I_{KN}$  in cultured PASMC. A, top, Effect of 10  $\mu\text{mol/L}$  anandamide on  $I_{KN}$  recorded during ramp, voltage protocol inset (left), and difference currents trace, obtained by subtracting current amplitudes in the presence of TASK-1 blocker from those obtained under control conditions (right). Difference current reversed close to  $-84$  mV, as expected for a  $\text{K}^+$ -selective conductance under these conditions. Bottom,  $I_{KN}$  evoked under symmetrical (155  $\text{K}^+$ ) conditions by ramp in the same cell (voltage protocol above), before (high- $\text{K}^+$ ) and during application of 10  $\mu\text{mol/L}$  anandamide (left) and difference currents trace (right). Difference current was voltage independent and reversed close to 0 mV, as expected for a  $\text{K}^+$ -selective conductance under these conditions. B, Concentration-response curve for anandamide.  $I/I_0$  is the current in the presence of anandamide expressed as a fraction of the current before anandamide application. The line is the best fit to the Hill equation using an  $\text{IC}_{50}$  of  $1.2 \pm 0.3$   $\mu\text{mol/L}$  and Hill coefficient of  $0.9 \pm 0.1$ . C, Effect of 10  $\mu\text{mol/L}$  anandamide on  $I_{KN}$  recorded at 0 mV. The current was markedly and reversibly inhibited during application of anandamide. D, Current-voltage relationship for whole-cell  $\text{K}^+$  current before and after application of 10  $\mu\text{mol/L}$  anandamide, activated from a holding potential of  $-80$  mV during 250-ms depolarizing pulses from  $-80$  to  $+70$  mV. Lines indicate voltage range used for conductance calculation by means of linear regression. The inset shows the kinetics of the anandamide-sensitive current.  $E_{\text{K-Nernst}}$  indicates Nernst equilibrium potential.

3D. Consistent with the blocking effect of anandamide on  $I_{KN}$ , a significant reduction in conductance resulted when anandamide was applied. Data are given in the Table.

The essential property of the TASK-1 channels is their extreme sensitivity to variations in extracellular pH ( $\text{pH}_o$ ) in a narrow physiological range. Figure 4A shows the  $\text{pH}_o$  dependence of  $I_{KN}$  of primary and cultured hPASMC across the full voltage range over which  $I_{KN}$  is apparent. Modification of  $I_{KN}$  by  $\text{pH}_o$  was reflected in resting membrane potential. A pH of 8.3 significantly hyperpolarized the cells, whereas acidification caused membrane depolarization in primary hPASMC ( $-10 \pm 1$  mV versus  $13 \pm 2$  mV;  $n=5$ ). Changes in whole-cell conductance caused by variation in  $\text{pH}_o$  in cultured hPASMC were significant (Table). Overall, we found a functional expression of kinetically and pharmacologically identical background  $\text{K}^+$  current carried by TASK-1 in both primary and cultured hPASMC. To provide more certain evidence for involvement of TASK-1 in  $I_{KN}$ , we tested the effect of tetraethylammonium (TEA) (10 mmol/L), 4-aminopyridine (4-AP) (3 mmol/L), ruthenium red (5  $\mu\text{mol/L}$ ), and different concentrations of  $\text{ZnCl}_2$  (online data supplement). As expected, TEA and 4-AP failed to inhibit  $I_{KN}$ . In contrast, ruthenium red caused a reduction of  $I_{KN}$ . However, the ruthenium red-sensitive current was linear and the reversal potential

varied between 0 and  $-20$  mV, where the calculated Nernst equilibrium potential was  $-84$  mV for  $\text{K}^+$ . It is well known that this compound is active at various sites (eg, ryanodine receptors<sup>10</sup> and TRPV channels<sup>11</sup>); therefore, this effect in primary hPASMC may not be surprising. The divalent zinc cation was also reported to inhibit TASK-1 at higher concentrations. However, in our study, the Zn-sensitive ion current had a reversal potential close to 0 mV, indicating the presence of a nonspecific leak current.

Taken together, both the potency of anandamide and pH 6.3 for blocking  $I_{KN}$ , and pH 8.3 for activating it, together with their effects on measured resting membrane potential ( $E_m$ ), strongly suggest that  $I_{KN}$  maintains the resting membrane potential in both primary and cultured hPASMC.

#### Modulation of $I_{KN}$ by Treprostinil

Prostaglandins possess a potent vasodilatory activity mediated by the stimulation of adenylate cyclase, with a subsequent increase in intracellular cAMP levels that is associated with the opening of  $\text{Ca}^{2+}$ -activated  $\text{K}^+$  channels ( $\text{K}_{\text{Ca}}$ ). The increased  $\text{K}^+$  conductance results in cell hyperpolarization and block of L-type  $\text{Ca}^{2+}$  channels, resulting in vasodilation. We used treprostinil, a stable prostacyclin analog, at a clinically relevant concentration, to test whether  $I_{KN}$  in hPASMC is also a treprostinil-sensitive conductance. As

**Conductances in Native and siRNA-Transfected hPASC**

Intervention	n	Conductance (nS)	P
<b>Native hPASC</b>			
Control (pH 7.3)	5	0.62±0.04	
pH 8.3	5	0.84±0.02	<0.001
pH 6.3	5	0.34±0.02	<0.001
Control (pH 7.3)	5	0.61±0.1	
Anandamide	5	0.39±0.1	<0.05
Control (pH 7.3)	6	0.61±0.04	
Treprostinil	6	0.89±0.02	<0.01
Anandamide+treprostinil	6	0.43±0.03	<0.01
Control (pH 7.3)	5	0.67±0.3	
KT 5720+treprostinil	5	0.72±0.4	NS
<b>siRNA-transfected hPASC</b>			
Control (pH 7.3)	5	0.41±0.1	
pH 8.3	5	0.44±0.2	NS
pH 6.3	5	0.40±0.2	NS
Control (pH 7.3)	5	0.41±0.1	
Anandamide	5	0.39±0.3	NS
Control (pH 7.3)	6	0.43±0.1	
Treprostinil	6	0.45±0.1	NS

illustrated by a single trace in Figure 5A, 10 nmol/L treprostinil enhanced  $I_{KN}$ , recorded at 0 mV (from  $10\pm 1$  to  $18\pm 2$  pA;  $n=6$ ;  $P<0.01$ ). The treprostinil concentration-response curve for TASK-1 in primary hPASC gave an  $IC_{50}$  of  $1.20\pm 0.11$   $\mu\text{mol/L}$  ( $n=4$ ; Figure 5C). Coapplication of 10 nmol/L treprostinil with 100 nmol/L iberiotoxin, a potent blocker of  $K_{Ca}$ , did not lead to a significant decrease in treprostinil-induced activation of  $I_{KN}$  (from  $11\pm 1$  to  $18\pm 2$  pA;  $n=5$ ;  $P<0.05$ ; online data supplement). Consistent with the involvement of TASK-1 channels in this activation, it was blocked when anandamide was previously applied earlier (online data supplement). Activation of TASK-1 with 10 nmol/L treprostinil was associated with 9-mV hyperpolarization of the resting membrane potential (from  $-42\pm 3$  to  $-51\pm 4$  mV;  $P<0.01$ ).

In rat tail artery smooth muscle cells, an activation of  $K_{Ca}$  by iloprost, another prostacyclin analog, was hypothesized to be mediated by cAMP-dependent PKA-induced phosphorylation of the channel.<sup>12</sup> To address the question of whether this pathway is important for TASK-1 activation by treprostinil, we chose a pharmacological approach to investigate the effects of PKA on  $I_{KN}$ . In whole-cell recordings, the direct application of the cell membrane-permeable cAMP analog 8-br-cAMP (an endogenous PKA activator) resulted in a significant increase of  $I_{KN}$  (from  $9\pm 2$  to  $17\pm 2$  pA;  $n=5$ ;  $P<0.05$ ; Figure 5D). The pretreatment of the cells with KT5720 (300 nmol/L), a specific inhibitor of cAMP-dependent protein kinase, abolished the effect of treprostinil on  $I_{KN}$  and on whole-cell  $K^+$  current, as shown in Figure 5E and the Table. We sought to investigate the effects of treprostinil exposure on the phosphorylation of TASK-1 in

hPASC. The PASC were incubated for 1 hour with 10 nmol/L treprostinil. No differences in the tyrosine phosphorylation of TASK-1 were observed when treprostinil-treated and untreated groups were compared (Figure 5F, top). In contrast, a 1-hour incubation with treprostinil (10 nmol/L) stimulated the serine/threonine phosphorylation of TASK-1, as was evident in TASK-1 immunoprecipitates probed with an anti-phospho(Ser/Thr) antibody (Figure 5F, middle). Protein loading equivalence was demonstrated by probing immunoprecipitates with an anti-TASK-1 antibody (Figure 5F, bottom). These results suggest that, in hPASC, TASK-1 channels are activated by treprostinil primarily through cAMP-dependent pathways.

**TASK-1 Knockdown Results in Depolarization of hPASC**

To further confirm the role of TASK-1 channels in regulation of  $E_m$  in hPASC, we knocked down TASK-1 expression in the cells using TASK-1 siRNA. Electrophysiological measurements were performed 24 to 48 hours after transfection of siRNAs. We found that the TASK-1 siRNA efficiently suppressed TASK-1 mRNA levels without affecting other widespread enzyme systems such as protein kinase C (PKC) (Figure 6A). The knockdown of TASK-1 caused a depolarization of resting membrane potential compared with the control cells ( $-26\pm 1$  mV versus  $-40\pm 2$ ;  $P<0.05$ ; Figure 6B). Pretreatment of hPASC with TASK-1 siRNA resulted in lack of significant further suppression of the  $I_{KN}$  by anandamide or acidosis as shown in Figure 6C (from  $3\pm 1$  to  $2\pm 1$  pA, from  $3\pm 1$  to  $3\pm 1$  pA, respectively). There was no significant activation by alkalosis or treprostinil (from  $4\pm 1$  to  $3\pm 1$  pA, from  $2\pm 1$  to  $2\pm 1$  pA, respectively). The whole-cell conductance in siRNA-pretreated cells was significantly lower, as illustrated in the Table. Changes in whole-cell conductance under variation of  $pH_o$  were not significant

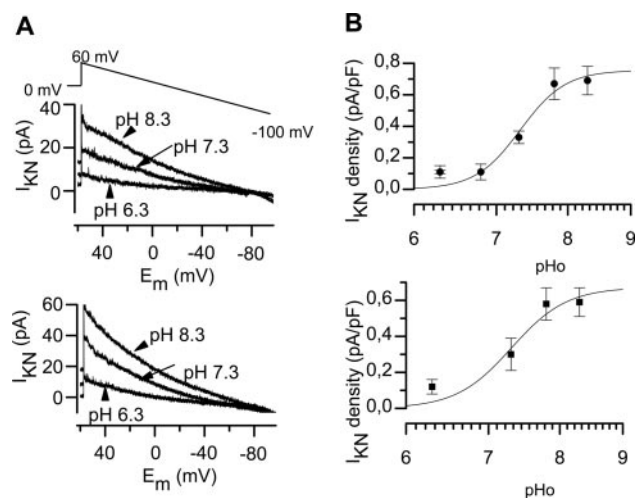


**Figure 4.** Modulation of  $I_{KN}$  by pH in primary and cultured hPASC. A, Representative time-course plot of  $I_{KN}$  at different  $pH_o$  in cultured (top) and in primary (bottom) hPASC recorded by ramp, activated from a holding potential of 0 mV during 1.6 second from 60 to  $-100$  mV. B, Relationship between  $pH_o$  and  $I_{KN}$  measured at 0 mV. Data were fit with a Boltzmann relationship with  $pH_{0.5}$  7.4 for cultured and  $pH_{0.5}$  7.3 for primary hPASC.

(Table). Modulation of  $I_{KN}$  by pH, anandamide, and treprostinil in hPASMC transfected with scrambled sequence TASK-1 siRNA are shown in the online data supplement.

### TASK-1 Is Inhibited by Acute Hypoxia in hPASMC

Because previous work implicated the TASK-1 channels as an important molecular component of the  $O_2$ -sensitive  $K^+$  current in PASMC, we investigated the  $O_2$  sensitivity of this channel in primary hPASMC. Representative traces recorded by ramp, before and after five minutes of exposure to hypoxic solutions, are shown in Figure 7A. The hypoxia-sensitive current reversed close to  $-84$  mV. Consistent with the involvement of TASK-1 channels in this inhibition, it was not further blocked when anandamide was additionally applied (Figure 7A). Under current-clamp conditions, hypoxia caused marked cell depolarization (by  $10 \pm 1$  mV;  $n=9$ ;  $P<0.05$ ). Pretreatment of hPASMC with TASK-1 siRNA resulted in lack of significant suppression of the  $I_{KN}$  by hypoxia (Figure 7B). Figure 7C summarizes the mean data confirming that hypoxia significantly inhibited TASK-1 in both primary and cultured hPASMC.

### Discussion

Smooth muscle cells have negative resting potentials that are important in regulating the excitability and contractile properties of tissues using these cells for force development. The resting membrane is regulated by  $K^+$  conductances that maintain the resting membrane potential close to the  $K^+$

equilibrium potential. At least 3 classes of potassium channels have been identified in PASMC: voltage-dependent potassium channels ( $K_v$ ),<sup>13-15</sup> calcium-activated potassium channels ( $K_{Ca}$ ),<sup>16,17</sup> and ATP-sensitive potassium channels ( $K_{ATP}$ ).<sup>18</sup> Although a new group of  $K^+$  channels, so-called background  $K^+$  channels, escaped detection at the molecular level for many years, it has now become clear that the newly identified KCNK family of  $K^+$  channel subunits also contributes to  $K^+$  current in smooth muscle cells.<sup>3,4</sup> When members of this superfamily of 2-PK channels are functionally expressed, they give rise to  $K^+$ -selective currents that are open at all voltages, in contrast to  $K_v$ ,  $K_{Ca}$ , or  $K_{ATP}$  channels whose activity is controlled by voltage or metabolic regulation. The decrease in this leak  $K^+$  conductance leads to cell depolarization that enhances the open probability of L-type  $Ca^{2+}$  channels in smooth muscle cells, causing periodic  $Ca^{2+}$  entry and vasoconstriction.

In this study, we demonstrated expression of TASK-1 mRNAs and proteins in human pulmonary artery smooth muscle cells. We found an anandamide-sensitive conductance in both primary and cultured hPASMC that had properties similar to TASK-1 channels. The native conductance showed an outward rectification in low external  $K^+$  solution, was instantaneous and noninactivating, was activated by alkalotic pH, and was blocked by anandamide. Transfection of TASK-1 siRNA into hPASMC significantly depolarized the resting membrane potential and abolished the effect of pH or anandamide. Furthermore, we were able to show the hypoxia sensitivity of the TASK-1 current. We conclude that TASK-1

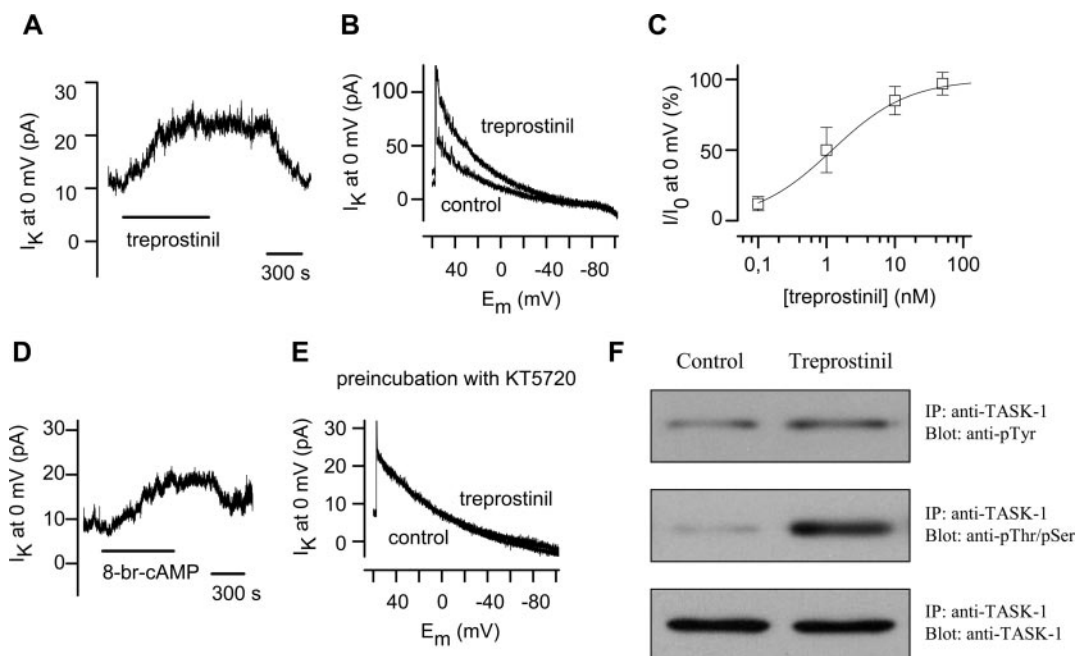


**Figure 5.** PKA-dependent activation of TASK-1 by treprostinil. A and B, Representative time-course plot of treprostinil application (10 nmol/L) on  $I_{KN}$  recorded at 0 mV in cultured hPASMC (A) and by ramp in primary hPASMC (B), activated from a holding potential of 0 mV during 1.6 second from 60 to  $-100$  mV. C, Concentration-response curve for treprostinil in primary hPASMC.  $I/I_0$  is the current in the presence of treprostinil expressed as a fraction of the current before treprostinil application. The line is the best fit to the Hill equation using an  $IC_{50}$  of  $1.2 \pm 0.1$   $\mu$ mol/L and Hill coefficient of  $0.9 \pm 0.1$ . D, Typical recording of the effects of the cell membrane permeable cAMP analog 8-br-cAMP (100  $\mu$ mol/L) on  $I_{KN}$  recorded at 0 mV in cultured hPASMC. E, Tyrosine (top) and serine/threonine (middle) phosphorylation of TASK-1 in treprostinil-treated and untreated (control) groups. Protein-loading equivalence is shown by probing immunoprecipitates with an anti-TASK-1 antibody in the bottom panel. Cultured hPASMC were used in D through F.

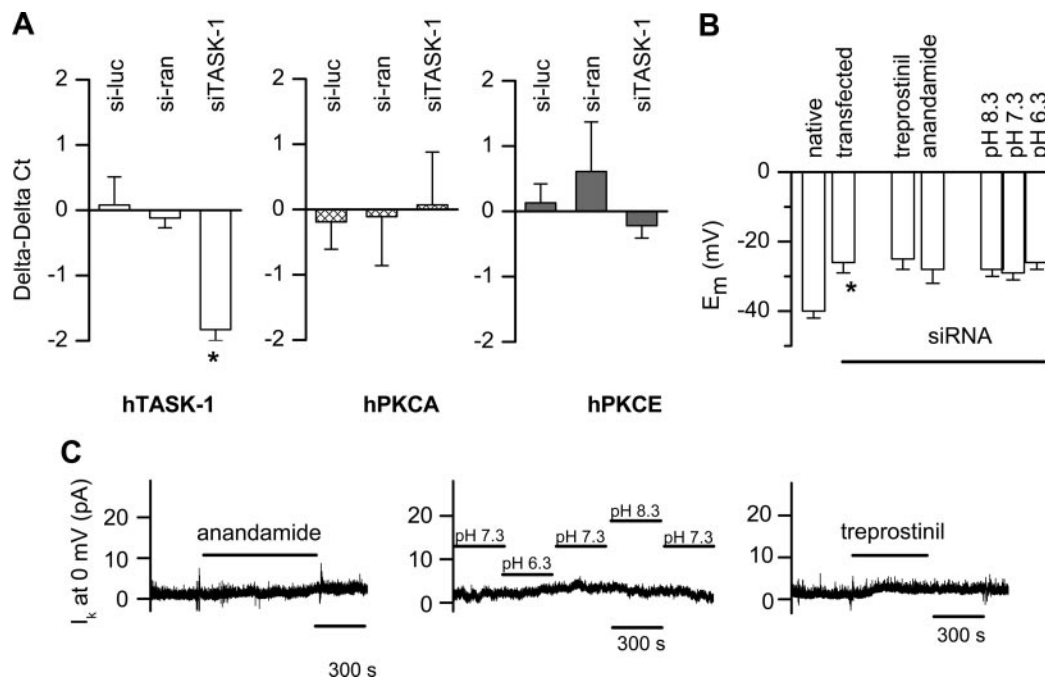


**Figure 6.** Lack of effect of anandamide,  $pH_o$ , and treprostinil on  $I_{KN}$  in siRNA-transfected hPASMC. **A**, Regulation of human TASK-1 (hTASK-1), human PKC $\alpha$  (hPKC $\alpha$ ), and human PKC $\epsilon$  (hPKC $\epsilon$ ) as measured by real-time RT-PCR (\* $P$ <0.05, 1-sample  $t$  test with  $H_0$ :  $\Delta\Delta Ct=0$ ). The  $\Delta\Delta Ct$  values are calculated as described in Materials and Methods. Positive values indicate upregulation of the target gene compared with control; negative values indicate downregulation. The  $\Delta\Delta Ct$  values are approximately proportional to the binary logarithm of the fold change. **B**, Resting membrane potential of native control and transfected cells shown left (\* $P$ <0.01). The  $E_m$  was significantly depolarized in transfected cells. Lack of changes in  $E_m$  under treprostinil, anandamide, or  $pH_o$  in transfected cells ( $n=5$  each group). **C**, Effect of 10 nmol/L treprostinil, 10  $\mu$ mol/L anandamide, and  $pH_o$  on remaining  $I_{KN}$  recorded at 0 mV.

channels are responsible for the hypoxia- and pH-sensitive, voltage-independent background conductance that sets the resting membrane potential in hPASMC.

The results of our experiments exclude the possibility that classical voltage-sensitive, Ca<sup>2+</sup>-sensitive, and ATP-sensitive K<sup>+</sup> channels play a significant role in mediating the observed pH-induced changes in the membrane potential. The sensitivity of  $I_{KN}$  to small changes in pH has been reported in many different cell types.<sup>2,19,20</sup> Local changes in pH caused by physiological or pathophysiological conditions such as hypo- or hyperventilation or ischemia in the pulmonary vascular bed may result in acidosis or alkalosis and lead to changes in pulmonary artery pressure. Our data suggest that effects on pH-sensitive ion channels may also explain the acidosis-induced vasoconstriction or the alkalosis-induced vasodilatory responses. Furthermore, anandamide, a selective blocker of TASK-1 significantly reduced the  $I_{KN}$  and caused a depolarization similar to that seen at pH 6.4. This is consistent with observations reported in earlier studies.<sup>3,9,21</sup> With a symmetrical K<sup>+</sup> distribution, anandamide inhibited a voltage-independent current with a reversal potential close of 0 mV, demonstrating the K<sup>+</sup> selectivity of the anandamide-sensitive current. To investigate the contribution of TASK-1 to whole-cell K<sup>+</sup> current, experiments were performed recording the whole-cell current from the holding potential of -80 mV, which allowed the acquisition of voltage-activated and background K<sup>+</sup> currents. Although the inhibitory effects of acidosis or anandamide were less pronounced, the endocannabinoid anandamide still caused a significant reduction in the cell conductance. Together, these data provide unequivocal

biophysical and pharmacological evidence for the functional expression of TASK-1 in both primary and cultured hPASMC.

The application of small interfering RNA provided further evidence to link resting membrane potential and TASK-1. The resting membrane potential and the cell conductances were significantly decreased in transfected cells. Moreover, the loss of the sensitivity of the membrane potential to significant depolarization by anandamide and pH 6.4, or to significant hyperpolarization by pH 8.4 in transfected cells, strongly implicates TASK-1 as a major contributor to the resting membrane potential.

Treprostinil, a stable analog of prostacyclin acts as a potent pulmonary vasodilator. In our experiments, treprostinil enhanced  $I_{KN}$  carried by TASK-1 in hPASMC. The current increase induced by treprostinil exhibited pharmacological saturation and reached a plateau as a consequence. Addition of 8-br-cAMP, a membrane-permeable analog of cAMP, exhibited similar effects. The activation of  $I_{KN}$  was still detected during coapplication of treprostinil with ITX, a selective blocker of Ca<sup>2+</sup>-activated K<sup>+</sup> channels, but treprostinil did not show any effect after pretreatment with anandamide. The activation of  $I_{KN}$  by treprostinil was abolished after preincubation with KT5720, an inhibitor of cAMP-dependent protein kinase. Moreover, our data indicate that treprostinil can stimulate the serine or threonine phosphorylation of TASK-1 and are consistent with the detection of phosphoserine in TASK-1<sup>22</sup> and the presence of consensus serine and threonine PKA and PKC phosphorylation sites in the TASK-1 peptide.<sup>2</sup> Whereas a tyrosine kinase consensus

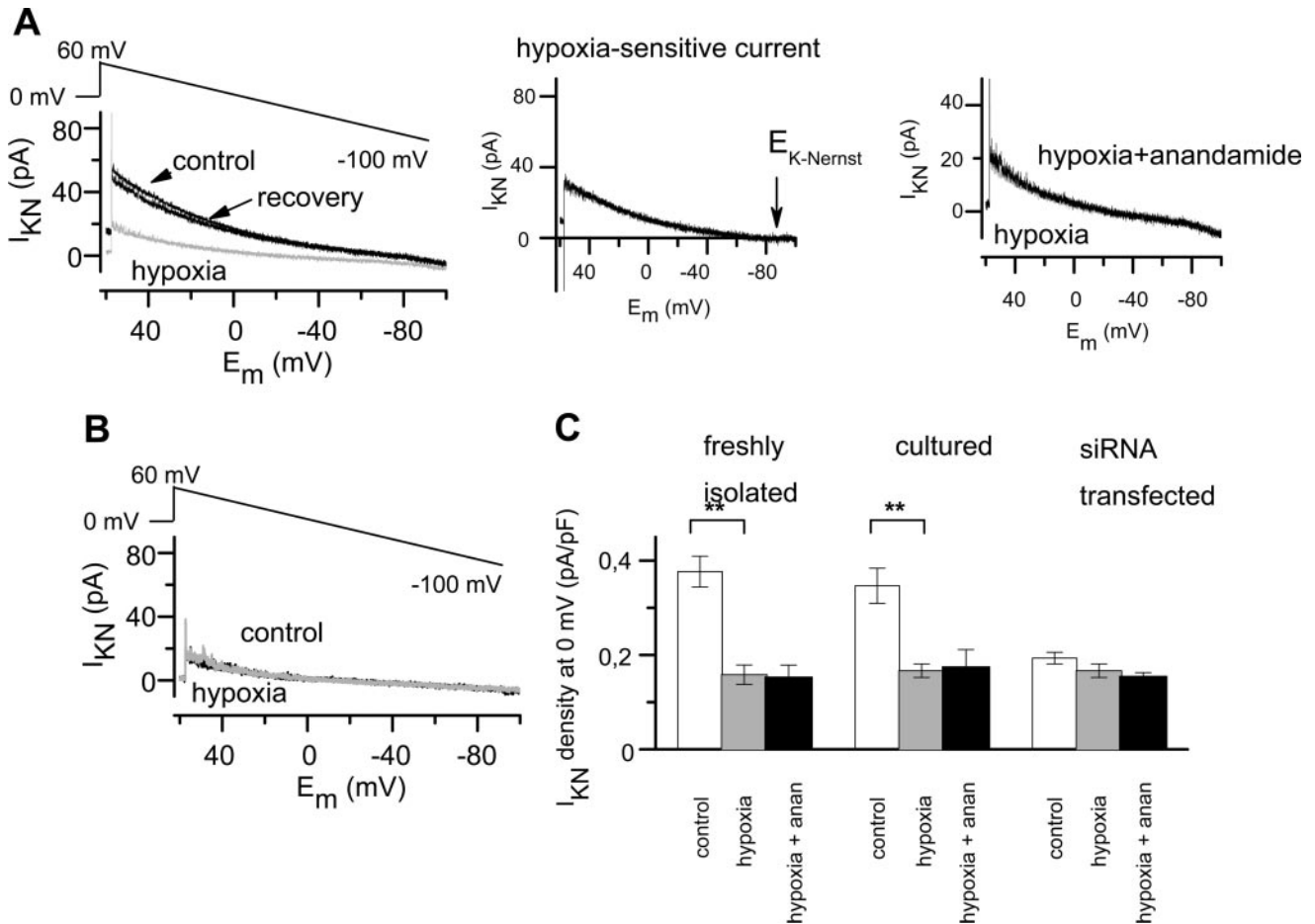


**Figure 7.** Hypoxia blocks TASK-1 in primary and cultured hPASMC. **A**, Effect of hypoxia on  $I_{KN}$  recorded by ramp in primary hPASMC (left) and difference currents trace, obtained by subtracting current amplitudes in the presence of hypoxia from those obtained under control conditions (middle). Difference current reversed close to  $-84$  mV, as expected for a  $K^+$ -selective conductance under these conditions. Application of  $10 \mu\text{mol/L}$  anandamide under hypoxic conditions did not cause a further change in the current (right), suggesting that the hypoxia-sensitive current is carried by TASK-1. **B**, Lack of hypoxia effect on  $I_{KN}$  in siRNA-transfected hPASMC. **(C)** Histogram summarizing the effect of hypoxia and anandamide (anan) under hypoxic conditions on  $I_{KN}$  calculated at  $0$  mV in primary, cultured and siRNA-transfected hPASMC ( $n=5$  each group;  $**P<0.01$ ).  $E_{K-Nernst}$  indicates Nernst equilibrium potential.  $E_{K-Nernst}$  indicates Nernst equilibrium potential.

site is also present in the TASK-1 peptide,<sup>2</sup> treprostinil did not effect tyrosine phosphorylation of TASK-1. There is accumulating evidence that intracellular protein kinases undertake important modulation of 2-PK channels. Members of the 2-PK superfamily such as TOK1 and TWIK-1 currents are potentiated by activators of PKC, whereas TREK-1 or TREK-2 currents are inhibited.<sup>23–25</sup> When human TASK-1 was expressed in *Xenopus* oocytes, the current was insensitive to activation of adenylyl cyclase by forskolin or IBMX.<sup>2</sup> In another study, the activation of PKA inhibited TASK-1 cloned from rat cerebellum,<sup>21</sup> whereas we observed PKA-mediated activation of TASK-1 by treprostinil and by 8-br-cAMP in hPASMC. This disparity in effects between these results could be related to clone specificity (human versus rat) or to preparations (oocytes versus native PASMC) with possible differences between cAMP levels and PKA activity.

Acute hypoxic inhibition of  $K^+$  channels is a critical step in regulatory processes designed to link lowering of  $O_2$  levels to cellular responses. It is often questioned whether the  $K^+$  channels are active at sufficiently negative potentials to set

the resting membrane potential of PASMC and whether  $K^+$  channels could mediate hypoxic pulmonary vasoconstriction. TASK-1 with the biophysical profile of a background  $K^+$  channel could be the perfect candidate for the initiation of hypoxia-induced depolarization in PASMC.

In conclusion, we demonstrated that TASK-1, a member of the 2-PK channel superfamily is expressed in human both primary and cultured hPASMC. TASK-1 controls the resting membrane potential, thus implicating TASK-1 channels in the regulation of pulmonary vascular tone. This channel is activated by c-AMP and may be one of the main targets for the beneficial action of prostanoids in therapy of pulmonary arterial hypertension.

### Acknowledgments

This study was supported by the Deutsche Forschungsgemeinschaft (SFB 547 “Cardiopulmonary Vasculature”). Excellent technical assistance from Brigitte Agari, Barbara Fröhlich, Sabine Gräf-Höchst, Christiane Hild, Esther Kuhlmann, Maria M. Stein, and Caroline Zörb is greatly appreciated.

## References

- Medhurst AD, Rennie G, Chapman CG, Meadows H, Duckworth MD, Kelsell RE, Gloger II, Pangalos MN. Distribution analysis of human two pore domain potassium channels in tissues of the central nervous system and periphery. *Brain Res Mol Brain Res*. 2001;86:101–114.
- Duprat F, Lesage F, Fink M, Reyes R, Heurteaux C, Lazdunski M. TASK, a human background K<sup>+</sup> channel to sense external pH variations near physiological pH. *EMBO J*. 1997;16:5464–5471.
- Gurney AM, Osipenko ON, MacMillan D, McFarlane KM, Tate RJ, Kempshall FE. Two-pore domain K channel, TASK-1, in pulmonary artery smooth muscle cells. *Circ Res*. 2003;93:957–964.
- Gardener MJ, Johnson IT, Burnham MP, Edwards G, Heagerty AM, Weston AH. Functional evidence of a role for two-pore domain potassium channels in rat mesenteric and pulmonary arteries. *Br J Pharmacol*. 2004;142:192–202.
- Osipenko ON, Evans AM, Gurney AM. Regulation of the resting potential of rabbit pulmonary artery myocytes by a low threshold, O<sub>2</sub>-sensing potassium current. *Br J Pharmacol*. 1997;120:1461–1470.
- Hong Z, Weir EK, Nelson DP, Olschewski A. Sub-acute hypoxia decreases K<sub>v</sub> channel expression and function in pulmonary artery myocytes. *Am J Respir Cell Mol Biol*. 2004;31:337–343.
- Vadasz I, Morty RE, Kohstall MG, Olschewski A, Grimminger F, Seeger W, Ghofrani HA. Oleic acid inhibits alveolar fluid reabsorption: a role in acute respiratory distress syndrome? *Am J Respir Crit Care Med*. 2005;171:469–479.
- Hsu K, Seharaseyon J, Dong P, Bour S, Marban E. Mutual functional destruction of HIV-1 Vpu and host TASK-1 channel. *Mol Cell*. 2004;14:259–267.
- Maingret F, Patel AJ, Lazdunski M, Honore E. The endocannabinoid anandamide is a direct and selective blocker of the background K<sup>+</sup> channel TASK-1. *EMBO J*. 2001;20:47–54.
- Hohenegger M, Suko J, Gscheidlinger R, Drobny H, Zidar A. Nicotinic acid-adenine dinucleotide phosphate activates the skeletal muscle ryanodine receptor. *Biochem J*. 2002;367:423–431.
- Guler AD, Lee H, Iida T, Shimizu I, Tominaga M, Caterina M. Heat-evoked activation of the ion channel, TRPV4. *J Neurosci*. 2002;22:6408–6414.
- Schubert R, Serebryakov VN, Engel H, Hopp HH. Iloprost activates K<sub>Ca</sub> channels of vascular smooth muscle cells: role of cAMP-dependent protein kinase. *Am J Physiol*. 1996;271:C1203–C1211.
- Post JM, Gelband CH, Hume JR. [Ca<sup>2+</sup>]<sub>i</sub> inhibition of K<sup>+</sup> channels in canine pulmonary artery. Novel mechanism for hypoxia-induced membrane depolarization. *Circ Res*. 1995;77:131–139.
- Weir EK, Archer SL. The mechanism of acute hypoxic pulmonary vasoconstriction: the tale of two channels. *FASEB J*. 1995;9:183–189.
- Platoshyn O, Remillard CV, Fantozzi I, Mandegar M, Sison TT, Zhang S, Burg E, Yuan JX. Diversity of voltage-dependent K<sup>+</sup> channels in human pulmonary artery smooth muscle cells. *Am J Physiol Lung Cell Mol Physiol*. 2004;287:L226–L238.
- Albarwani S, Robertson BE, Nye PC, Kozlowski RZ. Biophysical properties of Ca<sup>2+</sup>- and Mg-ATP-activated K<sup>+</sup> channels in pulmonary arterial smooth muscle cells isolated from the rat. *Pflügers Arch*. 1994;428:446–454.
- Peng W, Hoidal JR, Farrukh IS. Role of a novel K<sub>Ca</sub> opener in regulating K<sup>+</sup> channels of hypoxic human pulmonary vascular cells. *Am J Respir Cell Mol Biol*. 1999;20:737–745.
- Nelson MT, Quayle JM. Physiological roles and properties of potassium channels in arterial smooth muscle. *Am J Physiol*. 1995;268:C799–C822.
- Buckler KJ, Williams BA, Honore E. An oxygen-, acid- and anaesthetic-sensitive TASK-like background potassium channel in rat arterial chemoreceptor cells. *J Physiol*. 2000;525:135–142.
- Reyes R, Duprat F, Lesage F, Fink M, Salinas M, Farman N, Lazdunski M. Cloning and expression of a novel pH-sensitive two pore domain K<sup>+</sup> channel from human kidney. *J Biol Chem*. 1998;273:30863–30869.
- Leonoudakis D, Gray AT, Winegar BD, Kindler CH, Harada M, Taylor DM, Chavez RA, Forsayeth JR, Yost CS. An open rectifier potassium channel with two pore domains in tandem cloned from rat cerebellum. *J Neurosci*. 1998;18:868–877.
- O'Kelly I, Butler MH, Zilberberg N, Goldstein SA. Forward transport. 14–3-3 binding overcomes retention in endoplasmic reticulum by dibasic signals. *Cell*. 2002;111:577–588.
- Fink M, Duprat F, Lesage F, Reyes R, Romey G, Heurteaux C, Lazdunski M. Cloning, functional expression and brain localization of a novel unconventional outward rectifier K<sup>+</sup> channel. *EMBO J*. 1996;15:6854–6862.
- Lesage F, Guillemare E, Fink M, Duprat F, Lazdunski M, Romey G, Barhanin J. TWIK-1, a ubiquitous human weakly inward rectifying K<sup>+</sup> channel with a novel structure. *EMBO J*. 1996;15:1004–1011.
- Lhuillier L, Dryer SE. Developmental regulation of neuronal K<sub>Ca</sub> channels by TGFB1: an essential role for PI3 kinase signaling and membrane insertion. *J Neurophysiol*. 2002;88:954–964.

## Online data supplement

### Material and methods

#### *Preparation of human primary pulmonary artery smooth muscle cells (hPASMC) and cell culture*

Primary SMC were isolated from human pulmonary artery from three different nonused donor lungs, harvested for lung transplantation. The adventitia from small arteries with diameters of <1 mm was carefully removed under microscopic guidance and media pieces <1 mm<sup>3</sup> were placed onto 16-mm coverslips with 500 µl culture medium (Promocell Medium supplemented with penicillin and gentamicin; Promocell, Heidelberg, Germany). Cells were maintained at 37 °C, medium was initially changed after 24 h, and then every 48 h thereafter. PASMCs grown on coverslips were used for patch-clamp recordings within 6 days.

Cultured human PASMC from ten different donors were purchased from Cambrex (Walkersville, MD) or from Cascade Biologics (Mansfield, UK). Cells were maintained at 37 °C in smooth muscle growth medium (SmGM-2) containing nutrients from the SmGM Bullet kit (Cambrex, Walkersville, MD). Medium was initially changed after 24 h, and then every 48 h thereafter. Cells were sub-cultured, or plated onto 16-mm coverslips (for electrophysiological experiment) or in Petri dishes (for molecular biology studies) when 70 – 90 % confluent at passages 3–6.

SMC identity was verified by characteristic appearance in phase-contrast microscopy, The purity of PASMC cultures was confirmed using indirect immunofluorescent antibody staining for smooth muscle-specific isoforms of  $\alpha$ -actin and myosin (at least 95% of cells stained positive), and lack of staining for von Willebrand factor.

#### *Electrophysiology*

Cells were superfused at room temperature with bath solution of the following composition (in mmol/L): NaCl 140.5, KCl 5.5, CaCl<sub>2</sub> 1.5, MgCl<sub>2</sub> 1, glucose 10, Na<sub>2</sub>HPO<sub>4</sub> 0.5, KH<sub>2</sub>PO<sub>4</sub> 0.5, HEPES 10; adjusted to pH 7.3 with NaOH. High-K<sup>+</sup> - bath solution contained (in mmol/L): NaCl 10, KCl 155, CaCl<sub>2</sub> 1.5, MgCl<sub>2</sub> 1, glucose 10, Na<sub>2</sub>HPO<sub>4</sub> 0.5, KH<sub>2</sub>PO<sub>4</sub> 0.5, HEPES 10; adjusted to pH 7.3 with NaOH. The hypoxic bath solution was bubbled with N<sub>2</sub>. This procedure produced pO<sub>2</sub> values in the cell chamber of 24–30 mm Hg under hypoxic conditions (ABL TM510, Radiometer, Copenhagen, Denmark), pH was 7.40. Pipettes were filled with the following solutions: (in mmol/L): KCl 20, K-methanesulphonate (to suppress Cl<sup>-</sup> currents) 135, MgCl<sub>2</sub> 1, Na<sub>2</sub>ATP 2, ethyleneglycol bis(β-aminoethyl ether)-*N,N,N,N*-tetraacetic acid (EGTA) 1, HEPES 20; pH adjusted to 7.2 with KOH. Pipettes pulled from borosilicate glass tube (GC 150, Clark Electromedical Instruments, Pangbourne, UK) were fabricated on a model P-97 electrode puller (Sutter Instruments, Novato, CA, USA) and fire-polished to give a final resistance of 2 – 3 MΩ for whole-cell recording. To isolate *I*<sub>KN</sub> from other voltage-dependent K<sup>+</sup> currents, cells were clamped at 0 mV for at least 5 minutes as previously described {Gurney, 2003 1360 /id}. The effective corner frequency of the low-pass filter was 0.5-5 kHz. The frequency of digitization was at least twice that of the filter. No leak subtraction was made. The data were stored and analyzed with commercially available pCLAMP 9.0 software (Axon Instruments, Foster City, CA, USA).

### *Solutions and chemicals*

All compounds were purchased from Sigma Chemical Company (St. Louis, MO). Treprostinil was a gift from Lung RX (Satellite Beach, Florida, USA). All drugs were dissolved in experimental solution, with the exception of anandamide, which was dissolved in 50 (v/v)% ethanol in water. At this concentration the vehicle alone had no effect on K<sup>+</sup> current or resting

membrane potential. The pH of solutions containing drugs was tested and corrected to eliminate potential pH-induced effects.

### *Relative mRNA Quantitization*

Real-time PCR was used for relative quantization of the TASK-1, TASK-2, TASK-3, PRKCA, and PRKCE mRNA. Both GAPD and HMBS were used as reference genes (online table). The primers were designed to be intron-spanning where possible and maximal specific for the target genes. The reactions were performed in an ABI 7700 Sequence Detection System (Applied Biosystems, Foster City, CA) using SYBR-Green I as fluorogenic probe in 25  $\mu$ l reactions containing 2  $\mu$ l cDNA sample, 1 $\times$  qPCR<sup>TM</sup> Mastermix for SYBR Green I (Eurogentec, Seraing, Belgium), 45 pmol forward and reverse primer (see online Table 1). The cycling protocol was 1 $\times$  (50  $^{\circ}$ C, 2 min); 1 $\times$  (95  $^{\circ}$ C, 6 min); 45 $\times$  (95  $^{\circ}$ C, 5 s; 60  $^{\circ}$ C, 5 s, 73  $^{\circ}$ C, 10 s). The data for the amplification curves were acquired after the extension phase at 73  $^{\circ}$ C. After amplification, a melting curve was recorded and analyzed to identify possible contributions of unspecific products to the fluorescence signal. Additionally, an agarose-gel analysis was performed to confirm the primary formation of a single specific PCR product.

The background signal of the amplification curves was corrected for each gene individually using the signals recorded from cycle 3 to cycle 15-25, dependent on the onset of the exponential signal increase. The threshold value was set for each gene in the middle of the overlapping region of the exponential phases. Each gene was measured in duplicate in two independent experiments. The  $\Delta$ ct values for each target gene were calculated for both reference genes using the averaged ct values by  $\Delta$ ct = ct<sub>reference</sub> - ct<sub>target</sub>. The  $\Delta$ ct of the both reference genes were averaged and used to calculate the  $\Delta\Delta$ ct value by  $\Delta\Delta$ ct =  $\Delta$ ct<sub>siRNA</sub> -  $\Delta$ ct<sub>control</sub>. According to an amplification efficiency of approximately 2, the factors of differential target expression can be calculated by  $f = 2^{\Delta\Delta$ ct} (the efficiencies for the

amplification of the target genes have been determined in pilot experiments and were all greater than 1.98 or 98 %, respectively; data not shown). The error of the  $\Delta\Delta\text{ct}$  values was estimated from the average standard deviation of replicates using the error propagation by Gauss.

#### *Immunofluorescence staining*

Immunofluorescence was performed as previously described, using two different antibodies directed against unique domains of TASK-1, one at the amino terminus (Santa Cruz Biotechnology) and the other between residues 252 and 269 of the protein's carboxyl terminus (Alomone Labs) {Gurney, 2003 1360 /id}. hPASCs grown on glass slides were fixed for five minutes in cold methanol, rinsed five times in PBS. After blocking with 1% BSA overnight, cells were incubated with anti-TASK-1 antibody (1:50 dilution) for 1 hour then probed for 40 minutes with fluorescent labelled secondary antibodies (anti-goat IgG-FITC or anti-rabbit Alexa 555). Cells were counterstained with DAPI to identify the nuclear DNA. Duplicates were processed without primary antibodies for controls. Fluorescence was imaged with a Leica DM2500 M microscope, using Leica 40 (N.A. 1.0) objectives.

## Online Figure Legends

**Table 1 online: Primers used for quantitative real-time PCR**

Target Gene	Genbank Accession	Sequence 5' → 3'	Length (nt)	Exon <sup>1</sup>	Pos <sup>2</sup>	Amplicon Length (bp)
<i>TASK-1</i>	NM_002246	CGGCAAGGTGTTCTGCATG	19	2	440	91
		CAAGGTGTTGATGCGCTCG	19	2	512	
<i>TASK-2</i>	NM_003740	CCTTCATCACCATCTCCACCA	21	4	929	94
		TCCACGAAGTAGCGGTACAGG	21	5	1002	
<i>TASK-3</i>	NM_016601	GATGAAACGCCGGAAGTCC	19	2	1165	104
		AAATCCCGAAGCCGTGTTTC	19	3	1250	
<i>PRKCA</i>	NM_002737	GATGGATGGAGTCACGACCAG	21	13	1511	114
		AGGACGCCATAGGCCCA	17	14	1608	
<i>PRKCE</i>	NM_005400	CGGAAACACCCGTACCTTACC	21	10	1587	139
		GTGAACGAGGCTCGTCGAA	19	11	1707	
<i>GAPDH</i>	NM_002046	CGTCATGGGTGTGAACCATG	20	6	468	81
		GCTAAGCAGTTGGTGGTGCA	21	7	528	
		G				
<i>HMBS (PBGD)</i>	NM_000190.2	TGTCTGGTAACGGCAATGCG	20	1	153	70
		CCCACGCGAATCACTCTCAT	20	3	203	

<sup>1</sup>Number of the exon in which the primer sequence is located.

<sup>2</sup>Position of the 5' nucleotide of the primer relative to the Genbank sequence.

## Online Figure 1: Characterisation of $I_{KN}$ in primary hPASMCMC

(A) TEA (10 mmol/L) and 4-AP (3 mmol/L) failed to inhibit  $I_{KN}$  significantly. (B) Effect of ruthenium red (RR) on  $I_{KN}$  recorded during ramp in primary hPASMCMC (left), and “difference” currents trace, obtained by subtracting current amplitudes in the presence of ruthenium red from those obtained under control conditions (right). Difference current reversed close to 0 mV. (C) Effect of  $ZnCl_2$  on  $I_{KN}$  in hPASMCMC recorded during ramp, and “difference” currents trace (inset). Difference current reversed closed to 0 mV. Histogram summarizing the effect of different concentrations of  $ZnCl_2$  on  $I_{KN}$  calculated at 0 mV in cultured hPASMCMC (n = 4

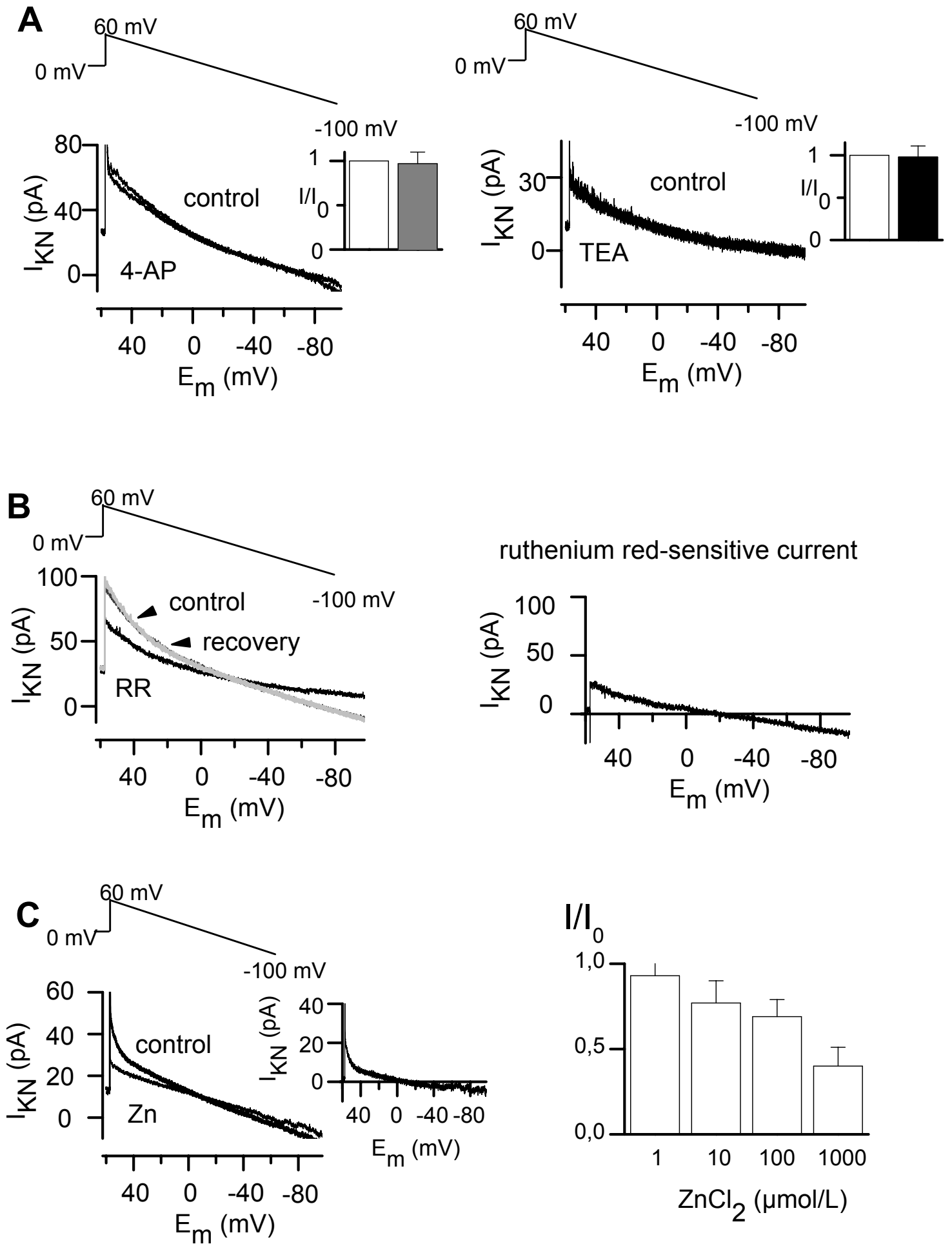
each group).  $I/I_0$  is the current in the presence of  $ZnCl_2$  expressed as a fraction of the current prior to  $ZnCl_2$  application.

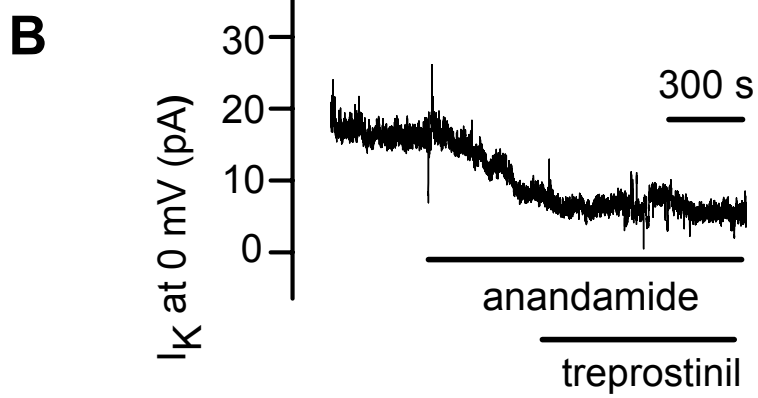
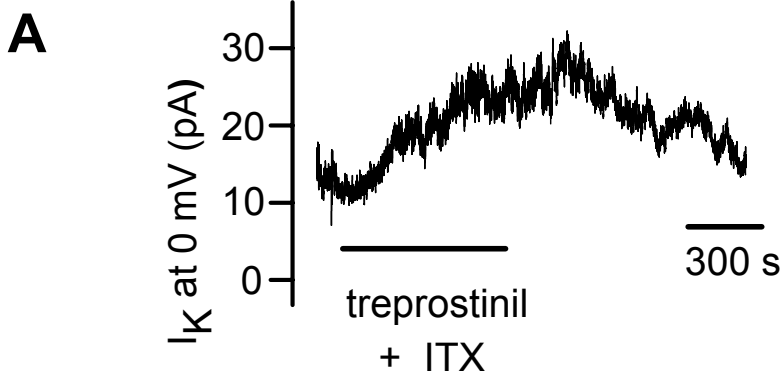
**Online Figure 2: Activation of  $I_{KN}$  by treprostinil**

(A) The activation of  $I_{KN}$  by 10 nmol/L treprostinil despite co-application of 100 nmol/L iberiotoxin (ITX). (B) After 10  $\mu$ mol/L anandamide pretreatment, treprostinil did not activate the current.

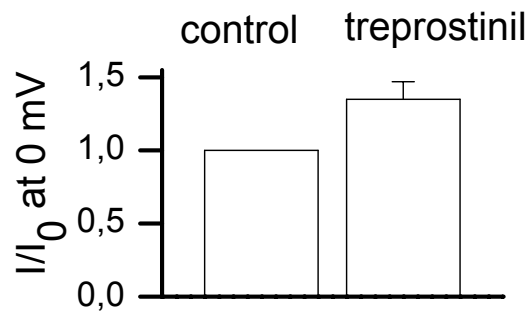
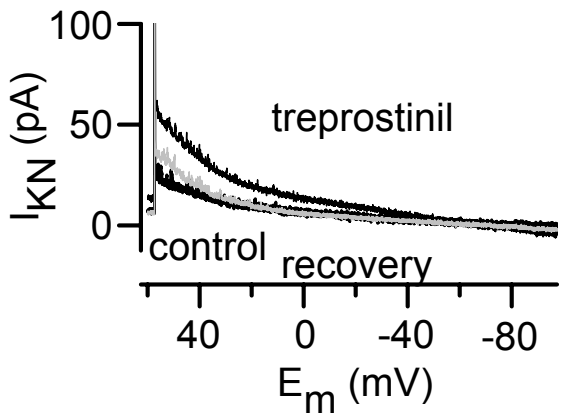
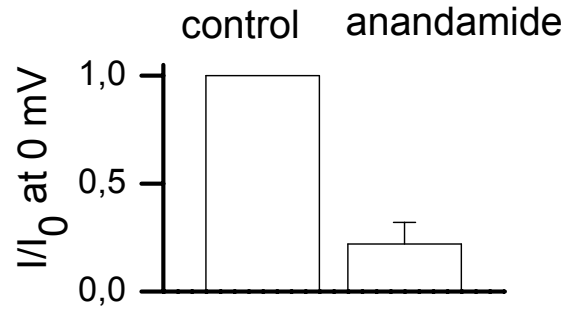
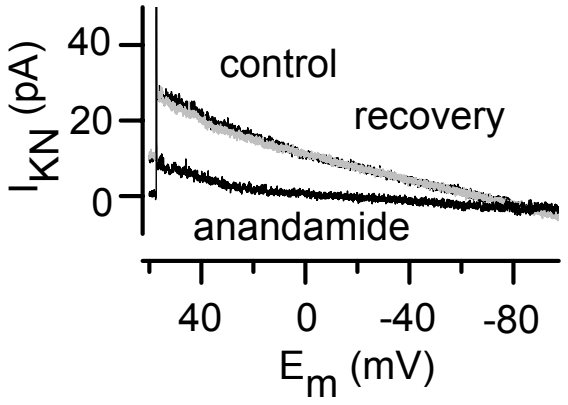
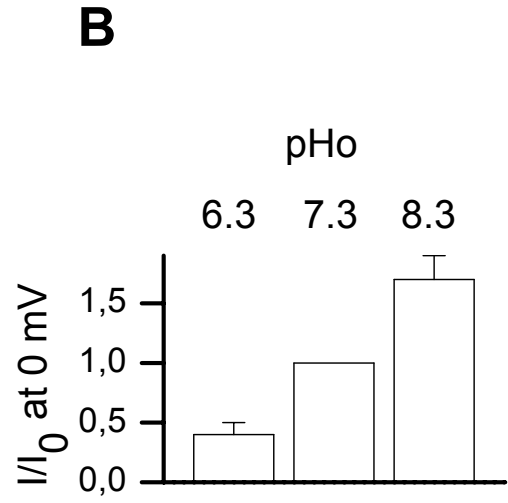
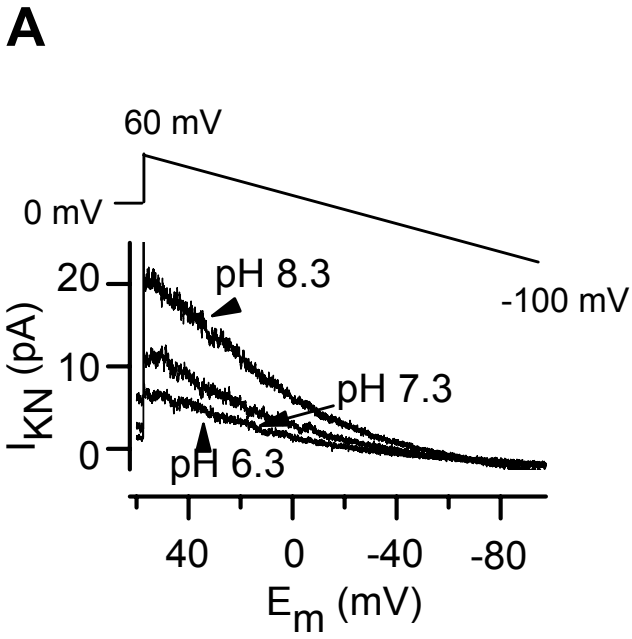
**Online Figure 3: Modulation of  $I_{KN}$  by pH, anandamide and treprostinil in cultured hPASMCM transfected with scrambled sequence TASK-1 siRNA**

Effect of  $pH_o$  (A), 10  $\mu$ mol/L anandamide (B) and 10 nmol/L treprostinil (C) on remaining noninactivating current ( $I_{KN}$ ) recorded at 0 mV in hPASMCM transfected with scrambled sequence TASK-1 siRNA.





**online-Fig. 2**



**online-Fig. 3**